STUDY OF THE GEAR RATTLE PHENOMENA IN AUTOMOTIVE POWERTRAIN SYSTEMS

Hugo Heidy Miyasato, hugomiyasato@gmail.com
Vinicius Gabriel Segala Simionatto, vinicius.simionatto@gmail.com
Milton Dias Junior, milton@fem.unicamp.br
Department of Mechanical Engineering, Faculty of Mechanical Engineering, State University of Campinas

Abstract. *The powertrain or driveline of automotive vehicles is the system responsible for transfering power from the engine to the wheels. Many of its noise, vibration and harshness (NVH) problems are detected only in late stages of the design chain, when all of its elements are tested together over a wide range of conditions. To attenuate the phenomena, only few changes are possible without resulting in very expensive palliative solutions. Once that engine and transmission are specified in early stages, satisfying power and torque modulation requirements, the only viable option left is the optimization of clutch parameters. In technical studies it has been verified that these characteristics, such as the stratified stiffness and hysteresis, have a great influence on the driveline dynamic behavior.*
Gear rattle is an impact induced-noise caused by the unloaded gear pairs of the gearbox. It is diagnosed with a higher intensity in diesel vehicle engines at low or idle speed, such as buses and trucks in a traffic jam, and in a more specific way found when a resonance for the whole driveline is excited. Creating low rattle level vehicles contributes also to the overall reduction of noise pollution in the cities.
In this work one representation of the clutch found in literature will be tested, and the torsional model response will be evaluated through numerical integration. Results from simulations with modifications on clutch parameters will be confronted with ones changing properties of other elements of the system, such as the flywheel inertia, gear backlash, and damping parameters of the gearbox in order to verify which approach provides results with a lower gear rattle level.

Keywords: *powertrain, gear rattle, nonlinear system*

1. INTRODUCTION

The term gear rattle makes reference to the sound induced by impacts between the unloaded gear mesh pairs in the transmission. It can be noticed on manual transmission vehicles in neutral condition (idle rattle) related to the engine firing frequency. Impacts occur with greater intensity on diesel vehicles, once that torque irregularities are increased with the adoption of this fuel. Rattle is also described in literature referring to a condition where high levels of vibrations are found in the transmission (drive rattle). For Drexl (1988), all automotive powertrains with manual transmissions have high levels of torsional vibration operating between 1000 and 2000 rpm, related to natural frequencies varying from 50 to 70 Hz in a linear characterization.

Heirichs and Bodden (1999) described gear rattle as an air borne sound, occurring when torsional vibrations of the gearbox are transmitted to its housing through the bearings. It also have a structure borne parcel, originated when the gearbox mounting system interacts with the vehicle frame. In some cases, the shifting system can contribute transmitting vibrations directly to the passenger cavity. In recent years a device called dual mass flywheel (DMF) has been used to reduce these vibrations, due to its inertial, stiffness, and damping effects (Albers, 1994). Instead of using a single flywheel inertia attached to the crankshaft, when a DMF is installed, the transmission input shaft inertia is increased, allowing better vibration insulation in both idle and drive rattle condition.

Singh *et al.* (1988) and Kim and Singh (2001) created nonlinear models to represent this phenomenon using a dead-zone nonlinearity to represent the gear backlash. Umezawa *et al.* (1986), based on experimental data, created an approximate curve for the simulation of helical gear pairs with time-variable mesh stiffness. Cai (1995), based on this previous work, incorporated geometric parameters such as the overlap ratio (ε) and transverse base pitch (X_z) to that formulation, enabling it to represent possible discontinuities on the total mesh stiffness due to the number of teeth in contact. The altered formula was applied for gear rattle simulations by Wang *et al.* (2001), Wang *et al.* (2002), Brancati *et al.* (2005) and Brancati *et al.* (2007).

In this work, Cai (1995) representation of the helical gear pair will be included on the model. The analysis of idle rattle will be taken with a systemic approach, testing also modifications on other system components. Natural frequencies of the linearized system in idle will be calculated and compared to the order content of the engine input torque. Then, a nonlinear model with piecewise linear stiffness and hysteresis representing the clutch and time-varying stiffness with backlash for the gears, will be subjected to alterations in clutch, gears and its inertial parameters in order to compare the gear rattle response in terms of vibration intensity.

2. NONLINEAR FUNCTIONS

2.1 Clutch

The clutch is the element which transfers power from engine to gearbox. Drexl (1988) defined that it enables a vehicle to start from standstill and it also allows interruption of power flow to stop and change gear. When the clutch is coupled to the flywheel, only its torsional vibration characteristics are representative. Equation 1 represents its piecewise linear stiffness torque function (T_k):

$$T_k(\Delta\theta) = \begin{cases} k_1\Delta\theta, & \text{for } |\Delta\theta| < \theta_{12} \\ sign(\Delta\theta)\left[k_1\theta_{12} + k_2(|\Delta\theta| - \theta_{12})\right], & \text{for } |\Delta\theta| > \theta_{12} \end{cases} \tag{1}$$

In Fig. 1a it is observable that, for low relative displacement between the flywheel and clutch hub ($\Delta\theta$), there is deformation of a torsional spring with very small elastic constant k_1. This stage is currently known in technical language as the idle stage, making reference to a stiffness characteristic. It is designed to be used when the vehicle is on neutral or idling condition, dealing with low values of engine torque. For situations when the clutch is engaged and a gear pair is selected transmitting torque to the wheels, above idle condition, the relative displacement becomes greater than a predefined transition angle θ_{12}. In this situation, a higher stiffness element k_2, also known as drive stage, is used to match the engine torque with the gearbox. Negative relative displacement, lower than $-\theta_{12}$, occurs when the torque of the rest of the powertrain is greater than the one provided by the engine. This stage is also known as coast.

There are friction elements inside the clutch in order to reduce the engine torque fluctuations. This characteristic is not only dependent by the relative displacement $\Delta\theta$, but also by relative speed $\Delta\dot{\theta}$. It is currently known as hysteresis function ($H(\Delta\theta, \Delta\dot{\theta})$) and is represented on Eq. 2. For low relative displacements ($|\Delta\theta| < \theta_{12}$), when only stiffness k_1 is transmitting torque from flywheel to clutch hub, the hysteresis is expressed as a constant therm with absolute value $H_1/2$ for positive and negative relative speed. When the system sets its operation point on higher stiffness element k_2, the hysteresis absolute value is greater ($H_2 - H_1/2$) for conditions of relative motion that cause greater deformation on drive ($\Delta\theta > \theta_{12}$ and $\Delta\dot{\theta} > 0$) or coast stage ($\Delta\theta < -\theta_{12}$ and $\Delta\dot{\theta} < 0$). Parameter H_2 must be greater than H_1 because the drive/coast stages deal with greater values of torque and its oscillations.

$$H(\Delta\theta, \Delta\dot{\theta}) = \begin{cases} \dfrac{H_1}{2}, & \text{for } \Delta\theta < -\theta_{12} \text{ and } \Delta\dot{\theta} > 0 \\ -H_2 + \dfrac{H_1}{2}, & \text{for } \Delta\theta < -\theta_{12} \text{ and } \Delta\dot{\theta} < 0 \\ \dfrac{H_1}{2}, & \text{for } |\Delta\theta| < \theta_{12} \text{ and } \Delta\dot{\theta} > 0 \\ 0, & \text{for } \Delta\dot{\theta} = 0 \\ \dfrac{-H_1}{2}, & \text{for } |\Delta\theta| < \theta_{12} \text{ and } \Delta\dot{\theta} < 0 \\ H_2 - \dfrac{H_1}{2}, & \text{for } \Delta\theta > \theta_{12} \text{ and } \Delta\dot{\theta} > 0 \\ -\dfrac{H_1}{2}, & \text{for } \Delta\theta > \theta_{12} \text{ and } \Delta\dot{\theta} < 0 \end{cases} \tag{2}$$

The clutch torque function (T_c) takes into account the effect of its elastic elements (T_k) and dissipative characteristics (H):

$$T_c(\Delta\theta, \Delta\dot{\theta}) = T_k(\Delta\theta) + H(\Delta\theta, \Delta\dot{\theta}) \tag{3}$$

Looking carefully to the representation of T_c on Fig. 1a, it is noticeable that H attributes an offset value of torque to T_k, plotted with a dashed trace. In operation, the effect of fluctuations in the engine torque is that the relative speed between flywheel and clutch hub varies abruptly from negative values to positive ones and vice versa, causing transitions from the upper and lower curves.

2.2 Backlash with a time-varying stiffness

Backlash (b) is the technical name given to clearances found between the gear tooth pairs (Fig. 1b). It occurs due to the dimensional tolerances chosen during the gear manufacturing stage, allowing also a proper lubrication of the contact surfaces. Low values of backlash are desirable, but it cannot be reduced significantly without component wear degradation. A piecewise formulation is used to represent backlash between the gear teeth as found in Eq. 4, graphically seen in Fig. 1c. The linear relative displacement is expressed by $\Delta x = r_p\theta_p + r_c\theta_c$, obtained from the pinion and crown gears pitch

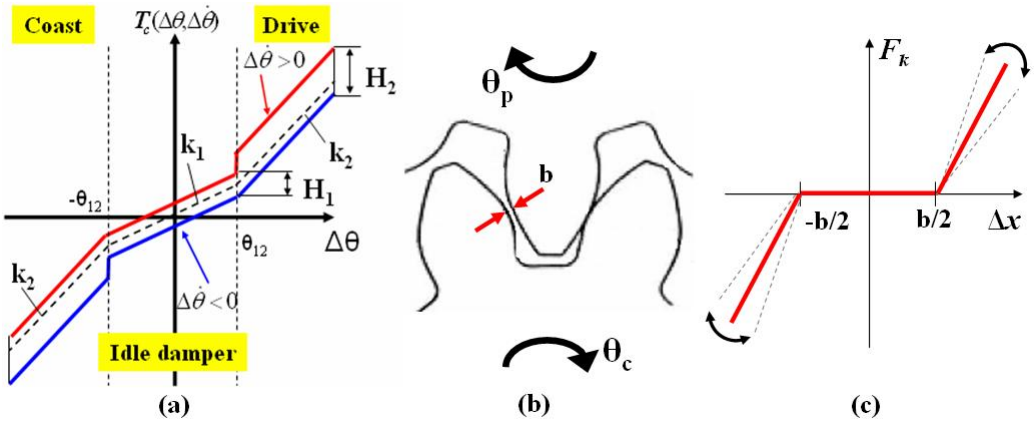

Figure 1. The clutch torque function is represented in Fig. 1a, taking into account the stratified stiffness and hysteresis function $H(\Delta\theta, \Delta\dot{\theta})$ (picture adapted from Kim and Singh (2001)). The linear backlash b is represented on Fig. 1b and its time-varying dead zone nonlinearity is shown in Fig. 1c (picture adapted from Wang *et al.* (2001)).

radius (r_p and r_c) and their angular displacements (θ_p and θ_c). The gearing relation is calculated from the relation r_p/r_c (Maitra, 1994) , which can be seen in Tab. 1.

$$F(X,\Delta x) = \begin{cases} 0, & \text{for } |\Delta x| < \dfrac{b}{2} \\ sign(\Delta x)\left[k(X)_{Total}\left(|\Delta x| - \dfrac{b}{2}\right)\left(\dfrac{3}{2}\gamma\Delta\dot{x}+1\right)\right], & \text{for } |\Delta x| > \dfrac{b}{2} \end{cases} \tag{4}$$

In Eq. 4, for low values of Δx, within the gap limits ($-b/2 < \Delta x < b/2$), the contact force is zero and each gear moves apart from each other. When this movement reaches its limits ($|\Delta x| = b/2$), the gear teeth are in contact and an impact occurs. For greater values of relative displacement, torque is transmitted by a time-varying stiffness $k(X)_{Total}$ related to the helical gear model. Energy dissipation was taken into account with a Hertz approach developed by Hunt and Crossley (1975). With this formulation, the energy loss is dependent on the deformation beyond the backlash limits ($|\Delta x| - b/2$) and the relative speed ($\Delta\dot{x}$). Parameter γ refers to the material and shape of contact bodies, causing modification on the coefficient of restitution in case of impact (Hunt and Crossley, 1975).

2.3 Helical gear stiffness

Cai (1995) derived an expression for the gear tooth stiffness from the work of Umezawa *et al.* (1986). The main gear geometric parameters involved are shown in Figure 2a. The plane of action is the one tangent to the gear base cylinders, where the meshing teeth promote a process of progressive contact and separation. A contact line represents the position of this movement evolving from the tooth base to its flank. At the same moment, more than one teeth is transmitting torque, each one at a different stage of the contact process, resulting in a representation on the contact plane made by contact lines of different lengths shifted by the transverse base pitch (X_z) along the line of action (X). The total length of contact (εX_z) is given by the total contact ratio (ε), obtained from the sum of the transverse (ε_α) and axial (ε_β) contact ratios ($\varepsilon = \varepsilon_\alpha + \varepsilon_\beta$). For one teeth pair only, the stiffness $k(X)$ was experimentally tested for the interval $1 < \varepsilon < 3$ along X, obtained from the absolute linear displacement of the pinion gear expressed by $X = r_p\theta_p$ (Brancati *et al.*, 2005):

$$k(X) = k_p exp\left(C_a\left|\frac{X-(\varepsilon X_z)/2}{1,125\varepsilon_\alpha X_z}\right|^3\right) \tag{5}$$

On the previous equation, k_p defines the peak value of that function, being directly proportional to the gear width (w). The coefficient C_a is dependent of the helix angle (β), width and tooth height (h), modifying the shape of the stiffness curve. Further details are provided on Cai (1995) and Umezawa *et al.* (1986).

The total contact ratio is related to the total number of gear pairs N in contact along the line of action. It is commonly found as a rational number, once that one of the pairs may be found with a contact of flanks, with a contact line that does not cross the whole width of the gear (Fig. 2a). In order to obtain the total meshing stiffness taking into account the contribution of every gear tooth pair, He *et al.* (2007) created a function which represents the fact that contact lines of gear pairs are shifted by X_z. Having it in mind, He *et al.* (2007) took advantage of the periodicity on the gear mesh stiffness curve, expressed on Eq. 6.

$$k_i(X) = k\left[(N-i)X_z + mod(X, X_z)\right], \text{where } mod(X, X_z) = X - X_z floor\left(\frac{X}{X_z}\right) \tag{6}$$

The total N of tooth pairs in contact was obtained approximating it by the nearest integer to ε (He *et al.*, 2007). Adopting one pair as reference on the plane of action (e.g. $i = 0$), the position of other tooth pairs i were calculated using the shifting term $(N-i)X_z$ in Eq. 6. The computational function "$floor$" rounds the division X/X_z by the lowest integer number near it (He *et al.*, 2007). As a result, $mod(X, X_z)$ describes the difference between the pinion gear displacement ($X = r_p\theta_p$) and the distance describing complete passages over the transverse base pitch (X_z). With this procedure, the position related to the value of $k_i(X)$ related to the pair i was obtained. To calculate the total gear mesh stiffness (Fig. 2b), it is necessary to sum the contributions of the N pairs that are simultaneously in contact along the line of action:

$$K(X)_{Total} = \sum_{i=0}^{N-1} k_i(X) \tag{7}$$

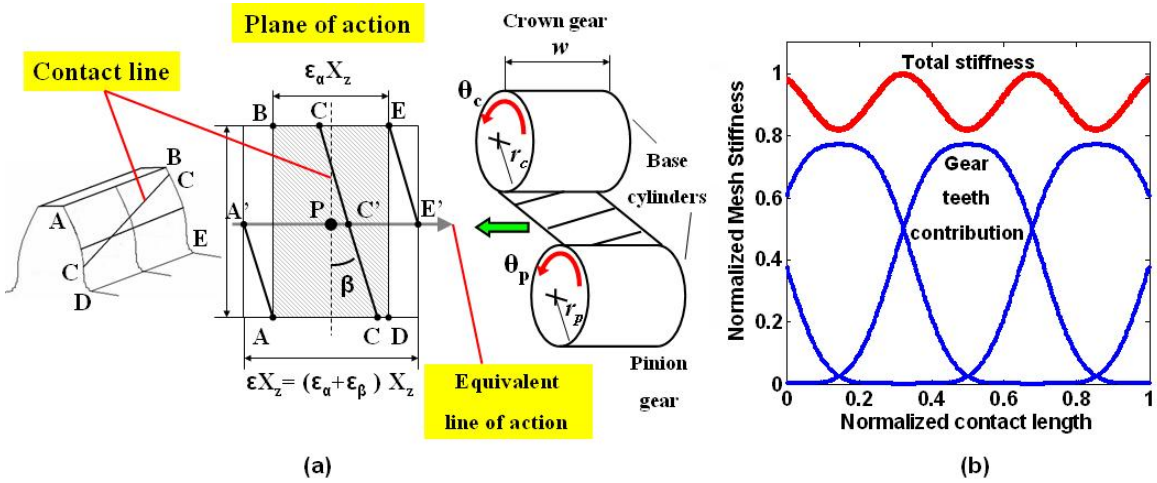

Figure 2. The plane of action formed between the meshing gears, emphasizing its main geometrical parameters is represented in Fig. 2a (picture adapted from Cai (1995)). Figure 2b shows the total mesh stiffness for the transmission fourth gear.

The total stiffness looks like a sinusoidal wave, coming from the fact that an helical gearing set provides a smoother contact than a spur one. This is one of the reasons why all gears from first to fifth gear in manual transmissions are helical. Following the same procedure for all gears, Tab. 1 shows their mean mesh stiffness, contact ratio and transverse base pitch. Since all pairs presented contact ratios on the interval $2 < \epsilon < 3$, there is no tooth separation during contact which could cause abrupt discontinuity on the total stiffness (Cai, 1995). This discontinuity is not related to the gear backlash. It occurs only when $2 < \epsilon$, meaning that, for specific moments of the contact process only one tooth pair is transmitting torque on the plane of action. For interpretation of the results obtained it is necessary to know that the unloaded gear inertia decreases from 1 to 5 gear.

Table 1. Gear pair standard characteristics for simulations.

Gear	r_p/r_c	**Inertia** (**kgm**^{2} $\times 10^{-3}$)	**Width** (**mm**)	**Helix** (°)	**Mean mesh stiffness** (k_t) (**N/m** $\times 10^8$)	**Contact ratio**	X_z (**mm**)
1	0.26	1.0	17.5	32	2,078	2,7913	18,1732
2	0.51	0.6	15.1	31.11	2,0838	2,8519	15,7416
3	0.64	0.5	14.55	30	2,4419	2,7565	17,1284
4	1.05	0.4	16.4	30	2,5456	2,8186	17,9452
5	1.32	0.25	15.2	30	2,4008	2,7415	17,0470

Figure 3a shows a strong face width (w) influence on the mean stiffness, once that k_p in Eq. 5 is directly proportional to it (Cai, 1995). The fourth gear pair with 60% of its original width could result in a mesh stiffness reduction from $2.54 \times 10^8 N/m$, with the standard w value, to $1.8 \times 10^8 N/m$, without changes in the helix angle. When w was varied

in nonlinear simulations, it was decreased from values shown on Tab. 1 because an increment on these standard values caused $\epsilon > 3$, trespassing the experimentaly tested range of the formula. This parameter can also modify ϵ (Fig. 3b) through ϵ_β (Maitra, 1994). Increase or decrease the helix angle results on much less modification in these curves.

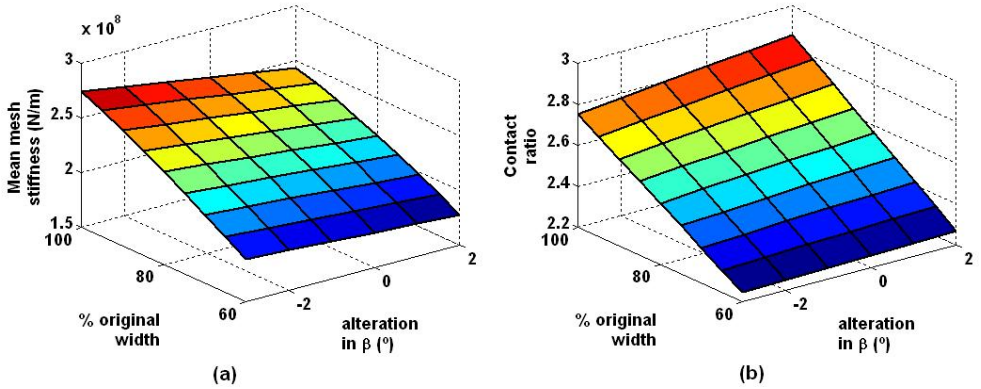

Figure 3. Figures 3a and 3b show the effect of the face width and helix angle in the mean stiffness and contact ratio, respectively.

3. DETAILED LINEAR MODEL AND ITS NATURAL FREQUENCIES

For a front wheel drive vehicle in neutral condition, the clutch is attached to the flywheel through a friction mechanism different from the one responsible for its dissipative effect with hysteresis. When a driver steps on the clutch pedal, the clutch is disengaged and, as consequence, there is no engine to transmission connection and *vice versa*. With a manual transmission, this process is required to allow the selection of one of its gear pairs. In order to transfer power to the wheels, one synchronizer is moved by the shifting system, making a desired gear move together with the output shaft. In idle condition, the clutch transfers torque generated by the engine firing sequence to the gearbox, and all unloaded gear pairs can be source of impacts, once that no synchronizer is selected. Figures 4a and 4b show a representation of the system in this condition and an idealization with lumped inertias.

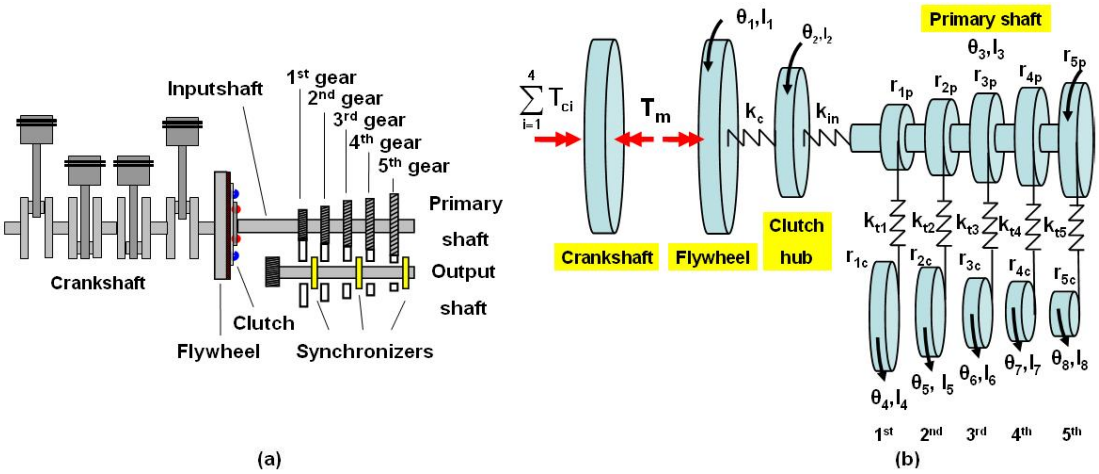

Figure 4. Representation of a front wheel drive powertrain in neutral condition and its linear model (Figures 4a and 4b).

In a rough representation, the crankshaft could be modeled as a single inertia excited by the sum of torques caused by the gas explosion on its cylinders. It interacts with the flywheel and the rest of the system through the torque T_m. With a proper consideration of T_m, the flywheel and the rest of the powertrain is studied separately from the engine model. This simplification avoids the greater complexity involved in including thermodynamics aspects as input for the model (e.g. cylinder pression curves representing combustion) interacting with the engine crank mechanism. It is commonly used in the area, employed also in all the works based on models consulted (Brancati *et al.* (2007), Couderc *et al.* (1998), Kim and Singh (2001), Singh *et al.* (1988), Wang *et al.* (2001) and Wang *et al.* (2002)). The effect of the engine is taken into account as an input torque T_m on the flywheel. A torsional spring k_c represents the clutch linearized on its idle stage, transmitting torque to the hub inertia, which moves the primary shaft through the inputshaft (k_{in}). Gear meshes from first to fifth gear are represented with a mean stiffness value (k_{ti}) obtained from Tab. 1.

Calculating the natural frequencies of the system excited by T_m, shown on Tab. 2, the first mode occurs at 0 Hz, representing a free-body mode arising from the absence of constraints with inertial references. It is remarkable that modes 4 to 8 are associated to higher frequencies, from 3129,9 up to 6424,4 Hz, strongly related to the fact that all gear meshes have very high stiffness values and small inertia on its unloaded gear (Table 1).

Table 2. Natural frequencies of the linear model in neutral condition.

Mode	1	2	3	4	5	6	7	8
Natural frequency (Hz)	0	5,4	478,0	3129,9	3670,5	3944,6	4187,4	6424,4

The spectral content for a four cylinder engine torque, whose main harmonics correspond to twice and four times its angular speed (order 2 and 4), is shown in Tab. 3. One can conclude that the idle rattle condition does not occur due to the excitation of a system vibration mode, once that its natural frequencies are positioned below the engine's second order (mode 2) and above the fourth order (modes 3 to 8).

Table 3. A four cylinder engine spectral content in idle condition.

Engine idle speed	**1st order**	**2nd order**	**4th order**
rpm	750-800	1500-1600	3000-3200
Hz	12,5-13,3	25-26,6	50-53,2

4. REDUCED NONLINEAR MODEL AND SIMULATIONS

In the previous section, it was observed that rattle in idle does not occur due to resonances excited in the powertrain system. It implies that this condition is strongly related to the nonlinear representation of its elements. A simplified nonlinear model with 4 degrees of freedom was created to study the influence and interaction between its main nonlinear functions. Each gear pair was simulated separately to evaluate the stiffness and inertial influence on the results as it can be seen on Fig. 5a (linearized) and 5b (nonlinear), for the 1st and 5th gear pairs, respectively. The highest natural frequencies obtained for this new linear representation from 1st to 5th gear were 3.25, 3.9921, 4.8283, 4.8286, and 4.9735 kHz. Comparing a nonlinear representation of Fig. 5b with the linear model in Fig. 5a the main differences rely on the representation of the clutch (stratified stiffness and hysteresis) and gearing (backlash with time-varying stiffness).

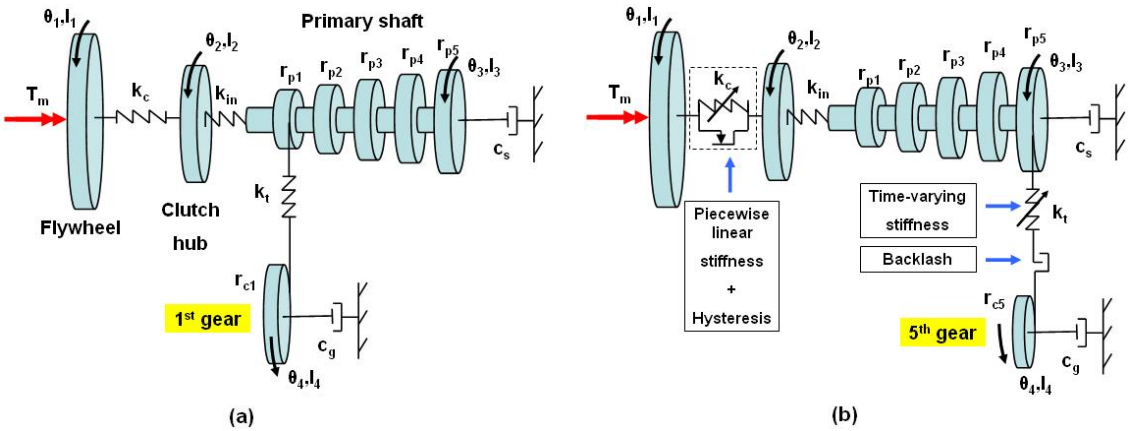

Figure 5. Representations of the linear and nonlinear model simulated for 1st (a) and 5th gear (b).

In all nonlinear simulations it was applied the torque function $T_m = 2 + 0,5sin(2\pi ft)$, with a frequency $f = 25$ Hz, corresponding to the second order of an engine with idle speed of 750 rpm. The mean value and the amplitude of the oscillatory component was obtained from the work of Wang *et al.* (2001).

All simulations were taken in Matlab ^{TM} environment with ode45 function. In order to achieve numerical stability during impacts, the relative error tolerance for all elements in solution vector was initially set to a minimum value of 10^{-6}. As the integration process evolved, this parameter was increased by the algorithm depending on the circumstances found. Solutions were obtained with a sampling period of 0.1 ms for the computation of spectral content up to 5 kHz.

Initially, clutch parameters (idle stage stiffness and hysteresis) were varied separately to verify their influence on the gear rattle behavior. Then, damping on the primary shaft was included, shifting its operation point. In this case, it was important to know the influence of the clutch transition angle on the gear pair vibration. In a next stage, gear parameters

such as backlash, helix angle and face width were varied. Finally, inertial properties of the system (flywheel and clutch hub) were altered. With these simulations, the powertrain is evaluated in a systemic approach, giving hints to engineers and designers about alternatives that could be effective to reduce gear rattle on a vehicle.

These sets of simulations generated significant data to be analyzed and compared. Padmanabham *et al.* (1995) created a rattle index (RI) based on the rms (root mean square) value of the unloaded gear acceleration signal, divided by the one obtained for the flywheel:

$$RI = \left\{ \frac{\ddot{\theta}_{gear,rms}}{\ddot{\theta}_{flywheel,rms}} \right\} \tag{8}$$

Table 4. Description of the simulations made varying parameters of the nonlinear model.

Element	Parameter varied	Gears tested
Clutch	Idle stage stiffness (k_1) / hysteresis (H_1)	1 to 5
	Transition angle (θ_{12})	5
Gear	helix angle (β) / face width (w)	1 to 5
Inertia	flywheel / clutch hub	1 to 5

5. RESULTS

5.1 Clutch parameters

The undamped model was tested for k_1 varying from 0.05 to 1.5 Nm/°. Commercial clutches for passenger cars have k_1 near 0.1 Nm/°. For all gears tested up to the commercial value, the rattle index was found below 40 (Figure 6a). Impacts resulted in RI growing from 1st to 5th gear, due to the reduction of inertia (Table 1). With $k_1 = 0.5$ Nm/° or more, the 5th gear presented RI over 80. These results suggests that a low value of k_1 and a higher inertia on the unloaded gear can reduce the vibration level of the impacts.

Then the influence of the idle hysteresis was taken into account, as shown on Fig. 6b with a different arragement of axes from Fig. 6a to ease the result's visualization, avoiding a covered view by the 5th gear results. The nonlinear model had no viscous damping and H_1 was varied from 0 to 0.4 Nm. The idle stage stiffness was maintained as $k_1 = 0.1$ Nm/°. For $H_1 = 0$ Nm, all gears presented higher values of RI, specially the 5th pair, with RI higher than 22. Including $H_1 = 0.1$ Nm of hysteresis to the model, all gears had their RI level reduced in comparison to the case with no hysteresis. Increasing this parameter to 0.3 and 0.4 Nm, the fourth and fifth gear pairs have presented very high levels of RI, greater than the ones found for $H_1 = 0$ Nm. This simulation group indicate an optimum value for H_1, once that it must exist to reduce the idle rattle vibration but a mistuned clutch can increase the level of impacts on the gearbox.

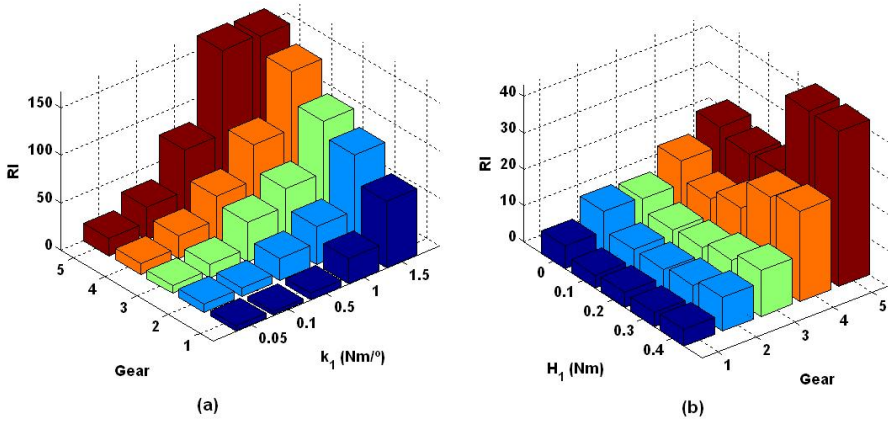

Figure 6. Rattle index for modifications in k_1 (a) and H_1 (b).

Setting the shaft viscous damping (c_s on Fig. 5) to 0.5 Nms/rad, simulating presence of drag torque, the clutch operation point is shifted. In Fig. 7 for H_1 equal zero or 0.1 Nm, the relative displacement between flywheel and clutch hub after 2s of simulation occurs around 4.16°. With a higher hysteresis ($H_1 = 0.4$ Nm) it is reduced to 3° after 6s. These results put evidence on the importance of choosing the clutch transition angle properly. If the operation point occurs nearby θ_{12}, the clutch may operate using both the idle and drive stiffness stages.

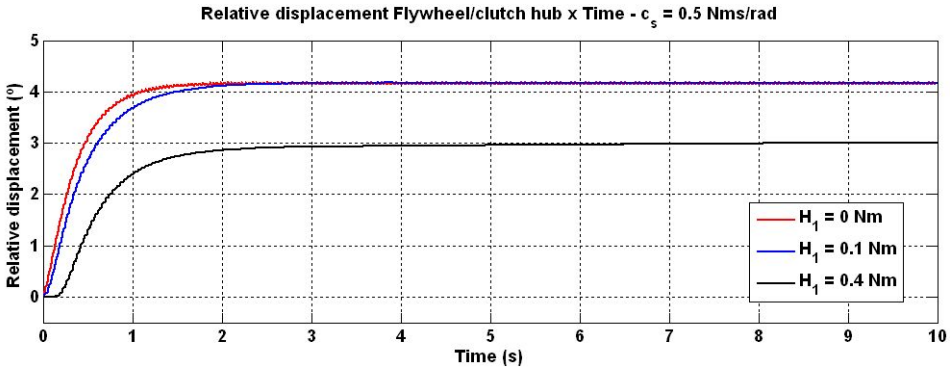

Figure 7. Relative displacement between the flywheel and clutch hub for $c_s = 0.5$ Nms/rad different values of H_1.

The transition angle (θ_{12}) was varied from 1 to 4.2° for $c_s = 0.5$ Nms/rad and $H_1 = H_2 = 0$ Nm. Figure 8a is made to understand how this clutch parameter influences the relative displacement between flywheel and inputshaft ($\Delta\theta$), causing modifications on RI. The upper and lower set of points, were obtained, respectively, from the difference of maximum and minimum values of relative displacement in regime ($Max(\Delta\theta)$ and $Min(\Delta\theta)$) with θ_{12}.

The rattle index value remains nearby 30 for simulations within the interval $1° < \theta_{12} < 3.6°$ (Figure 8b), when the clutch works with k_2 only (Figure 8a). RI grows as θ_{12} is increased, achieving a peak for $\theta_{12} = 3.9$ °, where both k_1 and k_2 are required for torque transmission (Figure 8a). Then, it decreases to very low values for $\theta_{12} = 4.2$ ° (Figure 8b), when the clutch works on its idle stage. These simulations indicate that the careless choice of θ_{12} may lead to the solicitation of the drive and idle stage stiffness, causing greater levels of RI than the ones obtained working with only k_1 or k_2.

For $\theta_{12} = 3.9°$, the clutch works on both idle and drive stages (Figure 9a). In Fig. 9c, it can be noticed that every time the drive stage is used, there is a peak of relative acceleration with negative signal marked with the letter D. As a result, stiffness k_2 makes the clutch hub reduce its speed dramatically, causing modification on the impact pattern between the negative and positive boundary (Figure 9b). In this case, impacts cause accelerations over 5000 rad/s^2 on the unloaded gear (Figure 9d).

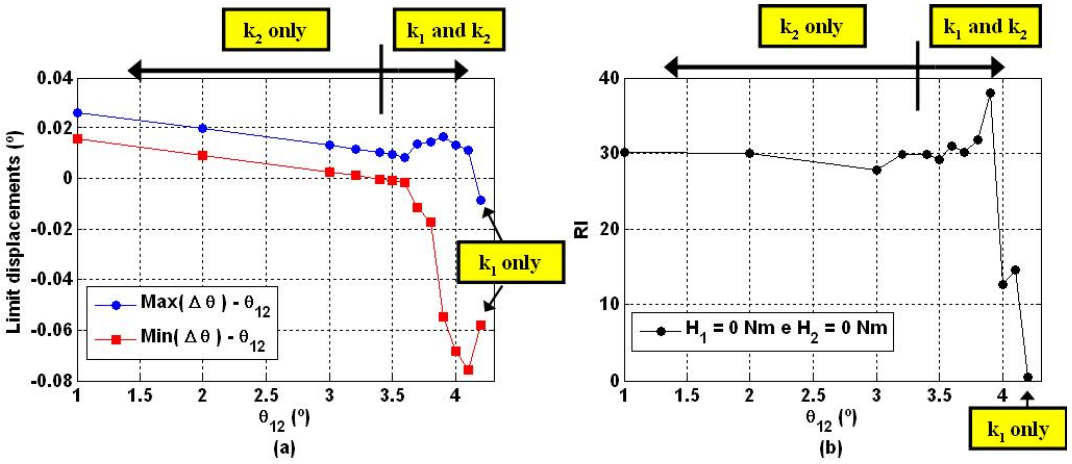

Figure 8. In *a*, the maximun and minimum deformation around the transition angle ($Max(\Delta\theta) - \theta_{12}$ and $Min(\Delta\theta) - \theta_{12}$) are shown for different values of θ_{12}. Rattle index for modifications in θ_{12} are represented in *b*.

5.2 Gear modifications

In this set of simulations, all gears had their standard helix angle (Table 1) increased by 2° and reduced by 3°. This parameter caused modifications in X_z, ε (Maitra, 1994), k_p and C_a (Cai, 1995) on Eq. 5. As it was shown on Fig. 3a, this parameter do not cause significant change on the mean mesh stiffness. As a result, it is not possible to identify any kind of pattern on Fig. 10a. The results show much more influence of the chosen gear pair on the RI level than its helix angle. For another simulation group, the influence of gear width was tested. It was reduced to 90, 80 and 70 % of the standard value (Table 1) causing greater mean mesh stiffness variation than the helix angle (Fig. 3a). Increasing this parameter resulted in $\varepsilon > 3$, out of the experimentally tested range for Eq. 5 (Cai, 1995). Lower values of w (70 and 80 %) resulted in high RI levels in Fig. 10b for the 4th and 5th gear.

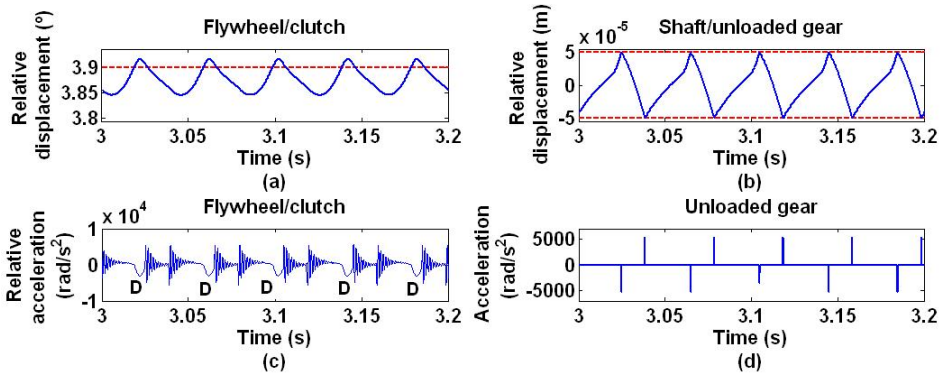

Figure 9. The relative displacement $\Delta\theta$ for $\theta_{12} = 3.9°$ can be seen in a. The relative displacement between the gear and shaft within the backlash is represented in b. Figure c shows the acceleration between flywheel and clutch hub. Acceleration on the gear due to impacts is represented on d.

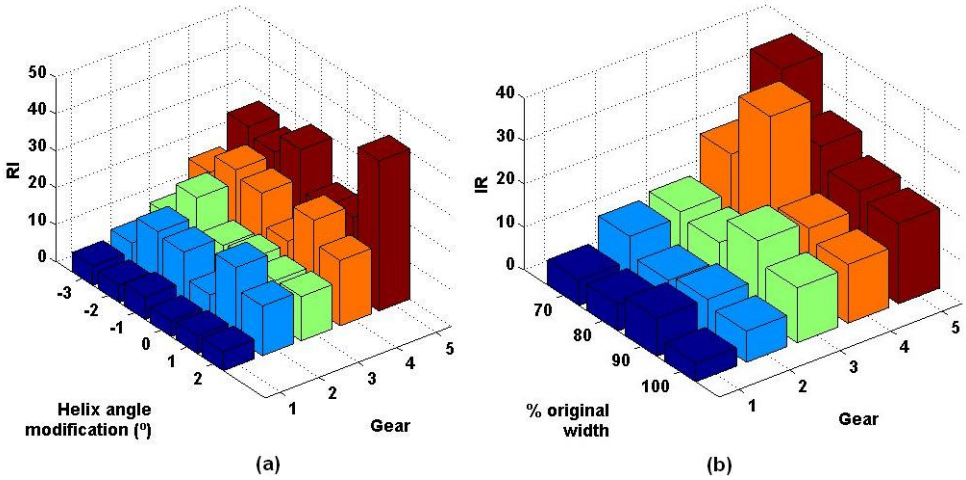

Figure 10. Rattle index for modifications on the gear helix angle (a) and width (b).

5.3 Inertial elements

The flywheel inertia was varied from 0.05 to 0.3 kgm^2 for 1st to 5th gear. In passenger cars, the real disk have an inertia around 0.1 kgm^2 (Brancati *et al.*, 2007). In Fig. 11a the RI value is reduced for all gears when its inertia is increased from 0.05 to 0.1 kgm^2 but, for grater values, there is no significant change on the system response. Modifying the clutch hub inertia from values 0.005 to 0.5 kgm^2 produced reduction on RI when the parameter is set to 0.1 kgm^2. It indicates that, with an inertia equivalent to the secondary mass of a dual mass flywheel device, there is significant reduction to all gears tested.

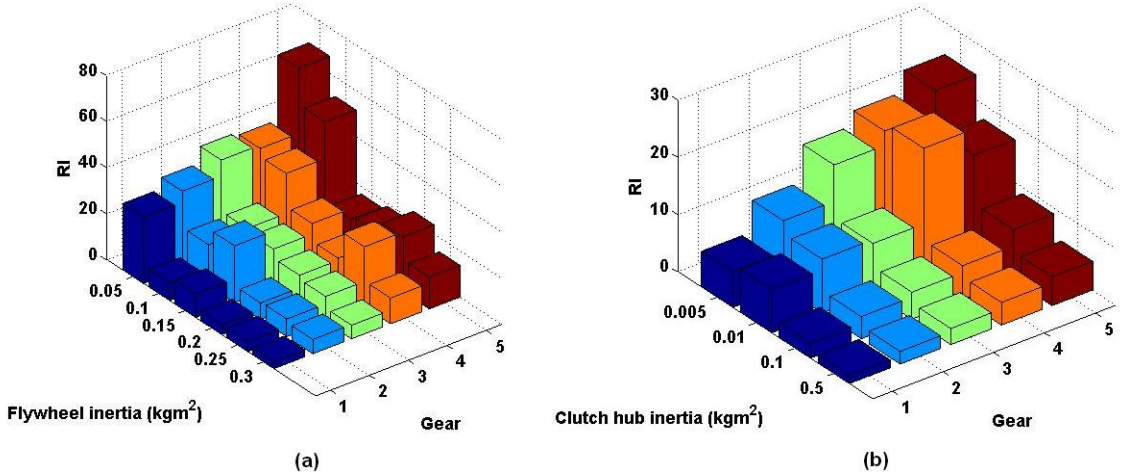

Figure 11. Rattle index for modifications in the flywheel inertia (a) and clutch hub (b).

6. CONCLUSIONS

The idle gear rattle is not caused by a vibration mode excitation of the driveline. There are no natural frequencies of the linearized model coincident with spectral content of the engine in idle condition. Modifications on the clutch stiffness parameter have strong influence on the gear rattle intensity, once that idle stage stiffnesses over 0.1 Nm/° have shown greater values of RI. The hysteresis seem to have an optimum range of values, resulting in vibration level increment when it is overdimensioned. Modifications on the stage transition angle resulted in greater level of vibration when the clutch worked on both idle and drive stages. Varying parameters such as the helix angle and gear width had small influence on the resultant impacts, which were much more related to the gear pair chosen. The unloaded gear pair of 4th and 5th gear presented the higher values of impacts in all simulations. Increasing the clutch hub inertia resulted in reduction of the RI level, showing the effectiveness of using a dual mass flywheel device on this system.

7. ACKNOWLEDGEMENTS

The two first authors are thankful to ZF Sachs do Brasil for the financial support and to Prof. Msc. Marco Antonio Zanussi Barreto for the technical support.

8. REFERENCES

Albers, A., 1994. "Advanced development of dual mass flywheel (dmfw) design". In *5th Luk Simposium*. Bühl,Germany, pp. 1–38.

Brancati, R., Rocca, E. and Russo, 2005. "A gear rattle model accounting for oil squeeze between the meshing gear teeth". *Journal Proceedings of the Institution of Mechanical Engineers, Part D: Journal of Automobile Engineering*, Vol. 219, No. 3–5, pp. 1075–1083.

Brancati, R., Rocca, E. and Russo, 2007. "An analysis of the automotive driveline dynamic behaviour focusing on the influence of the oil squeeze effect on the idle rattle phenomenon". *Journal of Sound and Vibration*, Vol. 303, pp. 858–872.

Cai, Y., 1995. "Simulation on the rotational vibration of helical gears in consideration of the tooth separation phenomenon (a new stiffness function of helical involute tooth pair)". *Transactions of the ASME, Journal of Mechanical Design*, Vol. 117, pp. 460–469.

Couderc, P.H., Callenaere, J., Hagopian, J.D., Ferraris, G., Kassai, A., Borjesson, Y., Verdillon, Y. and Gaimard, S., 1998. "Vehicle driveline dynamics behaviour: Experimentation and simulation". *Journal of Sound and Vibration*, Vol. 218, No. 1, pp. 133–157.

Drexl, H.J., 1988. "Torsional dampers and alternative systems to reduce driveline vibrations". *SAE Technical Paper*, , No. 870393, pp. 2.87–2.88.

He, S., Gunda, R. and Singh, R., 2007. "Effect of sliding friction on the dynamics of spur gear pair with realistic time-varying stiffness". *Journal of Sound and Vibration*, Vol. 301, pp. 997–949.

Heirichs, R. and Bodden, M., 1999. "Perceptual and instrumental description of the gear-rattle phenomenon". In *Proc. Int. Congress on Sound and Vibration*.

Hunt, K.H. and Crossley, F.R.E., 1975. "Coefficient of restitution interpreted as damping in vibroimpact". *ASME Journal of Applied Mechanics*, Vol. 97, pp. 440–445.

Kim, T.C. and Singh, R., 2001. "Dynamic interactions between loaded and unloaded gear pairs under rattle conditions". *SAE Technical Paper*, , No. 2001–01–1553.

Maitra, G.M., 1994. *Handbook of Gear Design*. Tata McGraw-Hill, New Delhi, India.

Padmanabham, C., Rook, T.E. and Singh, R., 1995. "Modeling of automotive gear rattle phenomenon: State of the art". *SAE Technical Paper*, , No. 951316.

Singh, R., Xie, H. and Comparin, R.J., 1988. "Analysis of automotive neutral grear rattle". *Journal of Sound and Vibration*, Vol. 131, No. 2, pp. 177–196.

Umezawa, K., Suzuki, T. and Sato, T., 1986. "Vibration of power transmission helical gears (approximate equation of tooth stiffness)". *Bulletin of JSME*, Vol. 29.

Wang, M.Y., Manoj, R. and Zhao, W., 2001. "Gear rattle modelling and analysis for automotive manual transmissions". *Proceedings of the Institution of Mechanical Engineers, Part D: Journal of Automobile Engineering*, Vol. 215, pp. 241–258.

Wang, M.Y., Manoj, R. and Zhao, W., 2002. "Numerical modelling and analysis of automotive transmission rattle". *Journal of Vibration and Control*, Vol. 8, No. 7, pp. 921–943.

9. Responsibility notice

The authors are the only responsible for the printed material included in this paper